

ARTICLE



Rightward brain structural asymmetry in young children with autism

Shujie Geng^{1,2}, Yuan Dai³, Edmund T. Rolls^{1,4,5}, Yuqi Liu³, Yue Zhang^{1,2}, Lin Deng³, Zilin Chen³, Jianfeng Feng^{1,2}, Fei Li³✉ and Miao Cao^{1,2}✉

© The Author(s), under exclusive licence to Springer Nature Limited 2025

To understand the neural mechanism of autism spectrum disorder (ASD) and developmental delay/intellectual disability (DD/ID) that can be associated with ASD, it is important to investigate individuals at an early stage with brain, behavioural and also genetic measures, but such research is still lacking. Here, using the cross-sectional sMRI data of 1030 children under 8 years old, we employed developmental normative models to investigate the atypical development of gray matter volume (GMV) asymmetry in individuals with ASD without DD/ID, ASD with DD/ID and individuals with only DD/ID, and their associations with behavioral and clinical measures and transcription profiles. By extracting the individual deviations of patients from the typical controls with normative models, we found a commonly abnormal pattern of GMV asymmetry across all ASD children: more rightward laterality in the inferior parietal lobe and precentral gyrus, and higher individual variability in the temporal pole. Specifically, ASD with DD/ID children showed a severer and more extensive abnormal pattern in GMV asymmetry deviation values, which was linked with both ASD symptoms and verbal IQ. The abnormal pattern of ASD without DD/ID children showed higher and more extensive individual variability, which was linked with ASD symptoms only. DD/ID children showed no significant differences from healthy population in asymmetry. Lastly, the GMV laterality patterns of all patient groups were significantly associated with both shared and unique gene expression profiles. Our findings provide evidence for rightward GMV asymmetry of some cortical regions in young ASD children (1–7 years) in a large sample (1030 cases), show that these asymmetries are related to ASD symptoms, and identify genes that are significantly associated with these differences.

Molecular Psychiatry (2025) 30:2860–2870; <https://doi.org/10.1038/s41380-025-02890-9>

INTRODUCTION

Autism spectrum disorder (ASD) is a typical neurodevelopmental disorder, that is difficult to effectively diagnose and treat due to its comorbidity with other neurodevelopmental disorders. Notably, ASD and developmental delay/intellectual disability (DD/ID) co-occur with a high prevalence of 68% [1–3], and both are highly heritable, with genetic causes contributing to 30–70% [4] and 25–50% of cases [5], respectively. The prevalence of DD/ID is estimated to be 1–3% in children under 5 years old [6]. It has now been recognized that atypical neural developments in the ASD population take place during the prenatal [7] to childhood stages [8–10], and symptoms appear before age 3 [11]. Revealing the comorbidities and differences between ASD and DD/ID in brain properties would be benefit for understanding the neuropathological mechanisms of both disorders. Notably, the human brain comprises a hierarchical system of multiple levels of organization from the microscale level including genetic and molecular processes, to the shaped morphology and dynamics of neurons and their synaptic connections at the mesoscale level, and the connected complex large-scale brain systems at macroscale level, which is a prerequisite for healthy brain function and complex

behavior. Examining how the distinct scales of nervous system organization may be potentially related could provide a better understanding to brain dysfunction. A substantial number of recent studies have investigated ASD-specific and shared pathological mechanisms with other neural developmental disorders in distinct scales, including the genetics, transcriptomes, neural imaging and behavioural performance in adults [12–16]. However, studies focused on the multiscale cascade of brain measurements in ASD and DD/ID during the early-stage of life, referring to how upstream gene expression affects hierarchical brain structure and function, ultimately leading to clinical manifestations are still lacking.

Left-right asymmetry is a fundamental organizing feature of brain structure and function and becomes specialized with development [17]. Structural and functional brain asymmetry have been reported to be heritable [18, 19]; to be genetically modulated [20–22]; and are established early in neonates [23], preterm infants [24] and even fetuses [25, 26]. In typically developing individuals, asymmetry measurements of brain asymmetry, including morphological indexes [27–29], functional and structural connectivity [30, 31], and topological properties of

¹Institute of Science and Technology for Brain-Inspired Intelligence, Fudan University, Shanghai, China. ²Key Laboratory of Computational Neuroscience and Brain-Inspired Intelligence (Fudan University), Ministry of Education, Shanghai, China. ³Developmental and Behavioral Pediatric Department & Child Primary Care Department, Ministry of Education-Shanghai Key Laboratory for Children's Environmental Health, Xinhua Hospital, Shanghai Jiao Tong University School of Medicine, Shanghai, China. ⁴Department of Computer Science, University of Warwick, Coventry, UK. ⁵Oxford Centre for Computational Neuroscience, Oxford, UK. ✉email: feili@shsmu.edu.cn; mcao@fudan.edu.cn

Received: 16 December 2023 Revised: 12 December 2024 Accepted: 7 January 2025

Published online: 15 January 2025

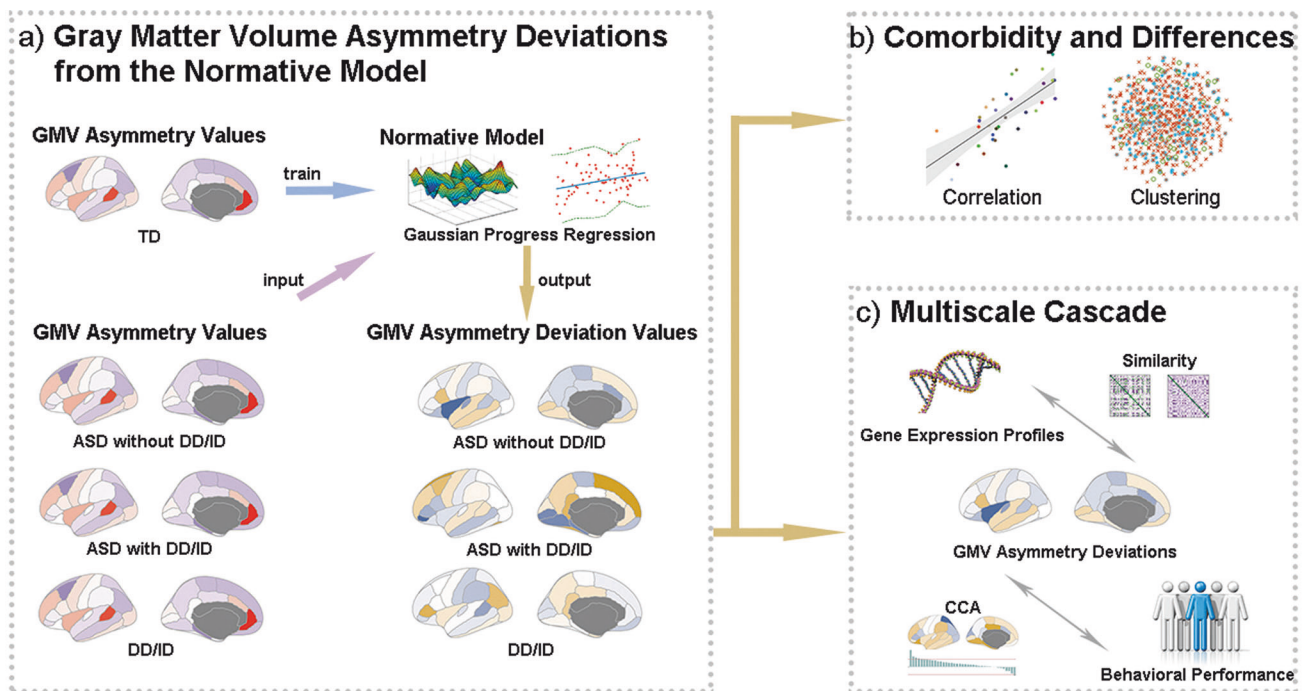


Fig. 1 Overview of the multi-scale cascade. **a** GMV asymmetry deviations in three atypical groups (ASD without DD, ASD with DD/ID, and DD/ID only) were extracted from a developmental normative model. The individual GMV asymmetry deviations were used to test the **b** comorbidity and differences across three atypical groups. **c** The multi-scale cascade was calculated by linking the GMV asymmetry deviations with the clinical symptoms and transcriptome profiles. ASD autism spectrum disorder, DD/ID developmental delay/intellectual disability, CCA canonical correlation analysis.

functional and structural brain networks [32, 33], were linked with functions of language, perception and action, emotion and decision making [34]. Notably, those functions were commonly impaired in ASD and DD/ID patients, suggesting that brain asymmetry has great potential as an intermediate neural phenotype linking genetic factors and clinical manifestations for those atypical populations.

Previous neuroimaging research revealed atypical brain asymmetry in populations with ASD. People with ASD showed reduced leftward structural and functional asymmetry in the frontal gyrus, superior temporal gyrus and other language-related regions compared with controls were linked to language impairments [35–38]. Specifically, Postema et al. investigated structural brain asymmetry in ASD patients based on a large sample recruited from the ENIGMA consortium, with 1774 ASD patients and 1809 controls, and found mild alterations in cortical thickness asymmetry in the medial frontal, orbitofrontal, cingulate and inferior temporal areas; surface area asymmetry in the orbitofrontal gyrus, and volume asymmetry in the putamen [39]. Notably, all outcomes had very low case-control effect sizes, which might be due to the group-level analysis methods, in which high heterogeneity would conceal the potentially informative features. Additionally, those studies mainly focused on older children with ASD and age-related effects were rarely considered. Moreover, research on brain asymmetry in DD/ID is lacking. How individual brain asymmetry at the early life stage is linked to gene expression and clinical manifestations and whether the relevant multiscale cascade could differentiate ASD and DD/ID from each other have not yet been investigated.

To answer these questions, we analyzed a large structural MRI dataset comprising 1030 children under 8 years old, including 775 children diagnosed with ASD (563 with DD/ID and 212 without DD/ID), 36 children with DD/ID only, and 219 typically developing (TD) children. We first assessed the mean values and distributions of the atypical individual deviations in gray matter volume (GMV)

asymmetry derived from the normative models for the ASD and DD/ID groups. Then, we employed canonical correlation analysis to explore the associations between asymmetry deviations and clinical and behavioural measures. Associations between atypical deviations in GMV asymmetry and transcriptional profiles were further explored with partial least squares (PLS) regression analysis and between-region similarity analysis. Gene annotations were interpreted through gene enrichment analysis (see the flowchart in Fig. 1).

METHODS

Participants

Participants were recruited from a neurodevelopmental project - Shanghai Autism Early Development Cohort [40]. All children were recruited from those who had visited the Department of Developmental Behaviour and Children Health Care, Xinhua Hospital, Shanghai Jiao Tong University, due to concerns of linguistic and/or social deficits and were assessed for early signs of autism. This study employed structural MRI data from 1030 young children. All children are Chinese, Asian. After imaging quality control (see below for details), the data of 1030 young children were employed for analysis, including 563 children diagnosed with ASD and DD/ID (3.98 ± 1.22 years, range from 1.26 to 6.93 years, 472 males), 212 children diagnosed with ASD without DD/ID (3.24 ± 1.15 years, range from 1.13 to 6.95 years, 184 males), 36 children with DD/ID only (4.42 ± 1.4 years, range from 1.26 to 6.8 years, 25 males) and 219 age-matched TD children (4.42 ± 1.62 years, range from 1.17 to 7 years, 107 males).

Clinical measurements, including scores of Autism Diagnostic Observation Schedule (ADOS), Childhood Autism Rating Scale (CARS), Autism Behavior Checklist (ABC), the Infant-Junior High School Life Ability Scale (SM), and Social Responsiveness Scale (SRS), and cognitive performance, scores of Gesell Developmental Schedules (GDS) or IQ measured by Wechsler Preschool and Primary Scale of Intelligence (WPPSI) and Wechsler Intelligence Scale for Children (WIS-R). The clinical diagnoses of ASD were made by pediatricians according to the *Diagnostic and Statistical Mental Disorders, Fifth Edition (DSM-5)* and ADOS or ADOS-toddler. To determine whether a child has DD/ID, his or her general intellectual ability was

assessed by the GDS for those younger than 4 years, WPPSI for those aged 4–6 years and WIS-R aged 6–7 years, with the GDS cut-off score <75 or a full IQ <70.

All patients completed ASD-related neurocognitive assessments, including the ADOS, CARS, ABC, and SRS. The total scores and subitem scores were used for subsequent analysis.

MRI data acquisition, quality control and processing

The MRI data of 283 children (164 ASD with DD/ID, 74 ASD without DD/ID, and 45 TD) were collected at site 1 with a Philips Ingenia MRI scanner. And MRI data of 747 children (399 ASD with DD/ID, 138 ASD without DD/ID, 36 DD/ID, and 174 TD) were collected at site 2 with a Siemens Verio MRI scanner. For the demographical details, please see Supplementary Table S1. Similar T1-weighted axial protocols were employed for structural MRI data collection. For the Siemens Verio scanner, the following parameters were used: repetition time (TR) = 2300 ms, echo time (TE) = 2.28 ms, flip angle = 8°, FOV = 192 mm * 192 mm; voxel size = 1*1*1 mm³; slice thickness = 1 mm, and slice number = 170. For the Philip Ingenia scanner, the following parameters were used: TR = 7.9 ms, TE = 3.5 ms, flip angle = 8°, FOV = 250 mm * 199 mm; voxel size = 1*1*1 mm³; slice thickness = 1 mm, and slice number = 170. To ensure collection, uncooperative children were sedated with chloral hydrate orally or by enema. Highly cooperative children were scanned in a resting state. The whole scanning procedure was conducted under the supervision of medical staff.

Raw structural images were independently manually inspected by two staff members (Dr. Y Dai and M.D. Y Liu) to exclude those with obvious motion artefacts. After quality control, the preprocessing steps included skull stripping, and realignment using CAT12 and then reregistered and segmented based on the Chinese pediatric atlases (CHN-PD) [41]. Then, we conducted the second round of quality control, comprising algorithms and a manual inspection of the segmentation results. Finally, smoothing using SPM12 with an 8 mm isotropic Gaussian kernel was conducted.

After preprocessing, we calculated the structural asymmetry metric employing the Desikan–Killiany template [42]. First, we coregistered the atlas to the CHN-PD and parcellated the preprocessed structural images of all subjects based on it. Then, the GMV for each brain region was calculated as the sum of voxel-wise intensities. Finally, the laterality index in each region for every subject was calculated as $\frac{GMV_{left} - GMV_{right}}{(GMV_{left} + GMV_{right})/2}$, which is a commonly used formula for values with a range from -2 to 2. The ComBat analysis based on an empirical Bayes approach was utilized to harmonize the site effects [43–45].

Statistical and normative modelling analysis

To generate the individualized abnormal asymmetry profiles of each region, we calculated the normative models of development using the Predictive Clinical Neuroscience toolkit [46] with the Gaussian process regression (GPR) method, which can provide point estimates as well as coherent measures of predictive confidence. Specifically, GPR models of GMV asymmetry for each ROI were trained based on 247 TDs with age and sex as covariates. Fivefold cross-validation was conducted to avoid overfitting and obtain optimal parameters. In this way, we generated developmental normative GMV asymmetry distributions in TD individuals. Then, we put the individual GMV asymmetry metric and covariate variables (age and sex) of children in the ASD with DD/ID, ASD without DD/ID and DD/ID only groups into the generated models and obtained the individual Z scores, which indicated the statistical estimate of the degree of deviation from TD distributions for each ROI of each subject.

To depict the group-specific profiles, we calculated the extents and distributions of asymmetry deviations for each atypical group. First, a one-sample *t* test was performed on deviation values for each group with a false discovery rate correction (FDR $q < 0.05$). Notably, a positive *t* value indicated that the corresponding ROI was more leftward lateralized compared with that of TD children, while a negative *t* value indicated increasing rightward asymmetry. In addition to testing the mean values, kurtosis of deviation values was also calculated. Considering that the kurtosis value of a standard normal distribution is 3, values above 5 were set as the threshold for abnormal criteria.

To investigate the categorical relationships among ASD and DD/ID populations, the similarities and differences in GMV asymmetry deviations among groups were then evaluated. Two-sample *t* tests were performed to capture between-group differences in mean values and kurtosis of deviation values of each region with FDR correction (FDR $q < 0.05$) for multiple

comparisons. Between-group similarity was calculated through Spearman's correlations across brain regions based on the group-averaged GMV asymmetry deviation values. To exclude the confounding effects of spatial autocorrelation [47, 48], spatial permutation analysis ($n = 10,000$ times) based on spherical rotations was conducted for each pair of diagnosis groups.

Clustering

To further investigate the relationships between patient groups, we conducted unsupervised clustering, *k*-means and *t*-distributed stochastic neighbor embedding (*t*-SNE) analyses using MATLAB internal functions. For *k*-means clustering, the summed between-group distances divided by the summed within-group distances were calculated as a function of cluster number *k*. The peak point of the generated ratio curve was selected as the optimal number of clusters, which indicated the highest homogeneity within groups with the lowest heterogeneity between groups. *t*-SNE is a nonlinear machine learning algorithm that converts high-dimensional data to a two-dimensional space for visualization. In this work, GMV asymmetry deviations in 34 regions for all subjects were imported into *t*-SNE to test whether subjects within the same diagnosis group were spatially gathered.

Associations with clinical and neuropsychological measurements

To understand the multiscale cascade in ASD and DD/ID populations, we conducted a canonical correlation analysis to explore the associations between brain structural asymmetry deviations and behavioural scores for ASD children without DD/ID and ASD children with DD/ID separately and jointly. The clinical measurements included body mass index; gestational weight; weight at birth; ABC score; and the ADOS, CARS, SM, SRS total and subitem scores. The neuropsychological measurements included the GDS scores or IQ scores. The clinical measurements and neuropsychological scores were put evaluated in canonical correlation analysis separately and jointly. Considering that age and sex were controlled as covariates in the normative model for GMV asymmetry deviation calculation, we did not include them here. The pairs of linear combinations of deviations in GMV asymmetry and clinical/neuropsychological measurements, known as canonical variables, were obtained. Then, we calculated the linear correlations of every original variable with the canonical variables, referred to as canonical loading, to determine their contributions. To exam the sample generalizability, the statistical significance of the identified CCA mode was tested through randomly permutating the rows in the original behavioral measurement's matrix 10,000 times with the GMV asymmetry deviation matrix untouched.

Associations with gene expression profiles

Estimation of regional gene expression profiles. Here, we employed the genome expression data of six postmortem neuro-typical human brains from the Allen Human Brain Atlas (AHBA) dataset (<http://human.brain-map.org>) to explore the associations between deviations in GMV asymmetry and relevant gene expression profiles [49]. We only used the transcriptional data from the left hemisphere considering that the available right hemisphere data were from only two donors. Traditional pre-processing of AHBA data was conducted according to the procedures in Arnatkevic et al. [50]. Then, the regional gene expression matrix (34*10,027, expression levels of 10,027 genes across 34 brain regions) was obtained for further analysis.

Partial least squares regression. We conducted the partial least squares regression (PLS) to investigate the effects of transcriptome profiles on the group-specific deviation patterns in GMV asymmetry [51]. Specifically, for each group, the gene expression matrix was used as the predictor variables while the statistic GMV asymmetry deviation values (*t* values from the one-sample *t* test) were used as response variates. A spatial permutation ($n = 10,000$) based on spherical rotations [47, 48] was performed to test the significance of the covariance among the PLS components, i.e., the linear combinations of transcriptome levels and deviations in GMV asymmetry [52, 53]. Then, we used Pearson's correlation to calculate the spatial similarity between the identified PLS components of gene expression and the GMV asymmetry deviation maps controlling the influences of spatial autocorrelation [47, 48]. Each gene's contribution to the maximally covariant PLS components was represented as the corresponding PLS weights, whose variabilities and significances were estimated through bootstrapping ($n = 10,000$) [52, 54, 55]. In this way, we obtained a list of genes that would be altered corresponding to the deviation patterns in GMV asymmetry for each atypical group ($p < 0.05$, FDR correction, two-tailed).

Inter-regional similarity analysis. Inter-regional similarity analysis was also conducted to calculate to explore the relationship between genetic expression and GMV asymmetry patterns. Here, we utilized Pearson's correlation to calculate the inter-regional similarity matrices (34×34) for gene expression profiles and deviations in GMV asymmetry separately. The lower triangle of the resultant matrices for each group was extracted as a vector. Then, the similarity between the vector of gene expression profiles and vector of deviations in GMV asymmetry was calculated with Spearman's correlation analysis for each diagnosis group. Spatial permutation ($n = 10,000$) tests were conducted to exclude spatial autocorrelation effects.

To further quantify the contribution of each gene to the results of inter-regional similarity analysis, a leave-one-out procedure was conducted. Specifically, each gene was removed, and the inter-regional similarity analysis was constructed based on the remaining genes. The difference between the new Spearman's correlation coefficient and the original Spearman's correlation coefficient was defined as the gene contribution index (GCI). To test the statistical significance of each GCI, bootstrapping ($n = 10,000$) with replacement of 10227 genes was performed to obtain the null distribution. The ratio characterized by the original GCI divided by the standard deviation of its null distribution was noted as the standard GCI score. Then, we ranked all genes by their standard GCI score and obtained an ordered, group-specific gene list.

Enrichment analysis. To explore the functional annotations of the gene lists for group-specific GMV asymmetry, we performed a meta-analysis for multiple gene lists based on the GO and the Kyoto Encyclopedia of Genes and Genomes (KEGG) on the Metascape website (<https://metascape.org/gp.inedx.html#/main/step1>). After extracting the top 1% of genes and the bottom 1% of genes from each ordered gene list, we uploaded the formed multiple gene list to the Metascape website, which has automated enrichment analysis tools with more than 40 independent knowledge bases. Then, the GO (biological processes, cellular components and molecular functions) terms and KEGG pathways enriched in each list were selected with FDR correction, $p < 0.05$.

RESULTS

Sample characteristics

We included a large sample of 1030 young children from the Shanghai Autism Early Developmental (SAED) Cohort [40], including 563 children diagnosed with ASD with DD/ID, 212 children diagnosed with ASD without DD/ID, 36 children with DD/ID only and 219 age-matched typically developing children. For age and sex distributions of all subjects, please see Supplementary Fig. S1 and Table S2. The clinical measurements were collected and statistically compared across the three patient groups and the TD group. Specifically, we found the following: (1) The cognitive performance, scaled by scores of Gesell Developmental Schedules (GDS) or IQ, of the three patient groups were significantly lower than those of the TD group; (2) The GDS or IQ scores of ASD with DD/ID and DD/ID children were also significantly lower than those of ASD without DD/ID children; (3) The two ASD groups had more severe social deficits than the TD and DD/ID groups. Bonferroni corrected, $P < 0.05$. For more details, please see Supplementary Table S3.

Atypical GMV asymmetry deviation patterns

We calculated the structural asymmetry metric employing the Desikan–Killiany template [42] for all subjects. The group averaged GMV asymmetry maps for the TD and three patient groups are shown in Fig. S2. Consistent with previous findings, similar structural lateralization patterns were found across the three patient groups and TD children. The superior temporal sulcus, rostral anterior cingulate and insula showed leftward laterality. The caudal middle frontal gyrus, parahippocampal gyrus, prefrontal gyrus and temporal pole showed rightward laterality.

We employed the Gaussian process regression (GPR) method to calculate the normative models of development in TD children and 5-fold cross validation to test the robust of normative model. Individual regional GMV deviations in 3 diagnosis groups were

then extracted from normative models trained by total TD children and each fold. The regional similarities across subjects between original GMV asymmetry deviations and each validation fold were shown in Fig. S3. The total brain GMV and regional GMV asymmetry developmental curves generated by the normative models were shown in Supplementary Fig. S4. The sexual mixed and sexual separate GMV lateralization deviation maps were shown in Fig. S5.

After then, we employed the one-sample t-test to detect regions with abnormal deviation values for each patient group (FDR corrected $p < 0.05$, Fig. 2a and Supplementary Table S4). Specifically, for ASD children without DD/ID, the inferior parietal lobe and precentral gyrus showed significant negative deviations, indicating more rightward asymmetry compared with normative children. Similar more rightward asymmetry pattern of these two regions was also observed in ASD children with DD/ID. Additionally, the rostral middle frontal gyrus showed significant positive deviations in ASD without DD/ID group, indicating more leftward asymmetry. Meanwhile, in ASD children with DD/ID, the fusiform and entorhinal were more rightward lateralized, and the isthmus cingulate, the bank of superior temporal sulcus, the paracentral gyrus, and the rostral anterior cingulate cortex were more leftward lateralized. Notably, no significant abnormality was found in any ROIs in children with DD/ID.

In addition to mean values, the kurtosis of regional deviation values within each patient group was calculated to explore the alterations of individual variability. Given that the kurtosis of the normal distribution is 3, a threshold of 5 was employed to detect the abnormality. As shown in Fig. 2b, 10 regions showed extreme kurtosis (entorhinal: $k = 64.391$; fusiform: $k = 31.153$; medial orbitofrontal: $k = 21.533$; parahippocampal gyrus: $k = 50.502$; postcentral gyrus: $k = 18.795$; precentral gyrus: $k = 16.193$; frontal pole: $k = 23.538$; temporal pole: $k = 41.451$; transverse temporal gyrus: $k = 16.145$) in the ASD without DD/ID group, indicating higher individual variations across subjects. For ASD children with DD/ID, the lateral occipital ($k = 12.203$) and temporal pole ($k = 32.759$) showed a changed distribution of GMV asymmetry deviations. The standard deviation (SD) and skewness of regional deviations were shown in Fig. S6. GMV lateralization deviation SDs of all ASD children fall into the SD distribution of TD children, showing no significant difference. The brain regions of ASD children showed abnormal skewness beyond the distribution of TD children were totally consistent with those measured by kurtosis higher than 5. Again, no regions in the DD/ID group showed altered kurtosis values (all kurtosis values < 5).

To make the functional annotations for the structural asymmetry deviation patterns, we calculated the mean Z values (normalized t values) and kurtosis values of functional systems with the Yeo-7 network template [56], as shown in Fig. 2c. Common atypical patterns of deviation values were found in the two ASD groups: abnormality in the default mode, ventral attention, somatomotor and visual networks. Also, the two ASD groups showed similar atypical distribution patterns with extreme high heterogeneity in limbic and visual networks.

To further explore the group differences, we conducted the two-sample t-test for comparisons between every pair of the patient groups and found no significant group differences for any region (FDR correction, $p < 0.05$). Spatial correlation analysis of GMV asymmetry across groups showed significant similarity between the ASD with DD/ID vs. ASD without DD/ID groups ($r = 0.557$, permuted $p = 0.0007$) and the ASD with DD/ID vs. DD/ID groups ($r = 0.741$, permuted $p < 0.0001$), as shown in Fig. 3a. Additionally, we employed the unsupervised clustering algorithms to explore whether the patient groups could be separated from each other based on the GMV asymmetry patterns. Using the k-means method, we calculated the distance ratio, as the summed distance between clusters divided by the summed distance within clusters, with number of clusters ranging from 2 to 20. No peak

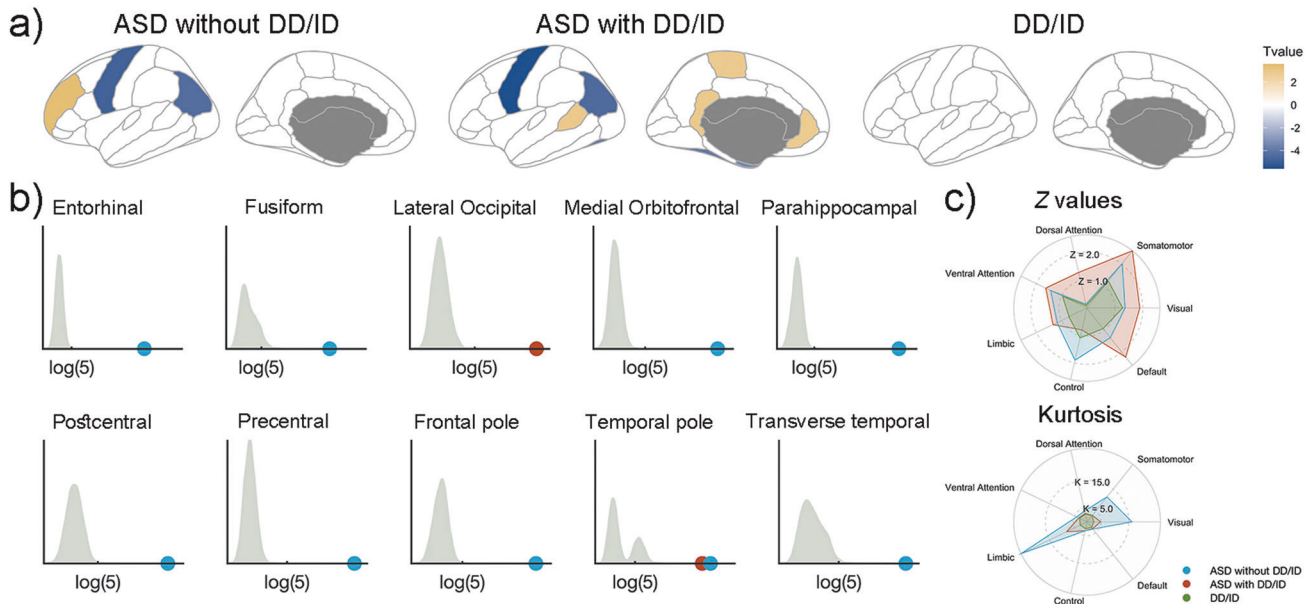


Fig. 2 The GMV asymmetry deviations in the three patient groups. **a** The brain regions with significantly altered GMV asymmetry deviations characterized by one-sample *t* test in the three patient groups. **b** The brain regions with abnormal GMV asymmetry deviation distribution in ASD patients with and without DD/ID. The grey areas of the histograms show the kurtosis distribution of GMV deviations in TD children. The red and blue dots show abnormal kurtosis in ASD children with DD/ID and ASD children without DD/ID, respectively. **c** The average *Z* values and kurtosis in Yeo's 7 networks. The *t* value in each brain region was transformed into a *Z* value and used to calculate the average *Z* value for each network. Red indicates ASD children with DD/ID, blue indicates ASD children without DD/ID, and green corresponds to children with DD/ID only. ASD autism spectrum disorder, DD/ID developmental delay/intellectual disability.

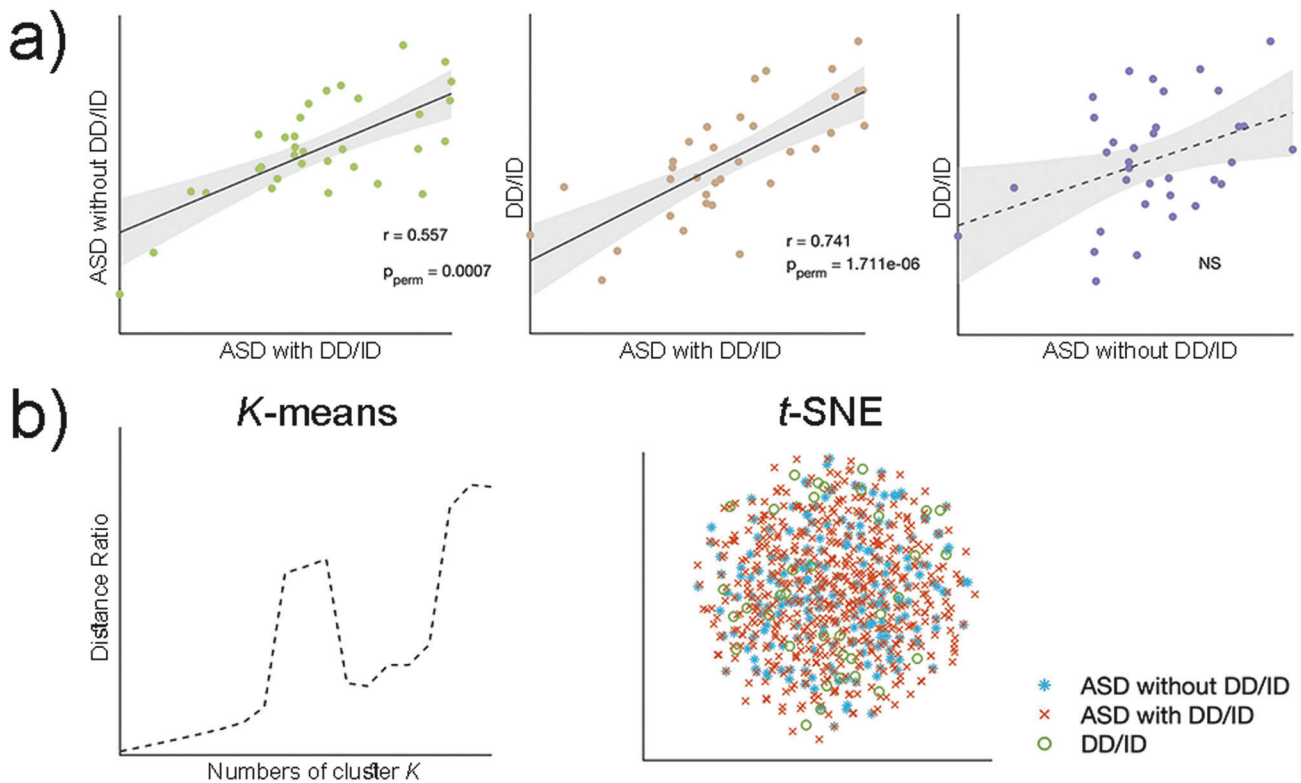


Fig. 3 Comorbidities between patient groups. **a** Spearman correlations of whole-brain GMV asymmetry deviations between any two patient groups. Significantly similar GMV asymmetry patterns were found in ASD with DD/ID v.s. ASD without DD/ID groups and ASD with DD/ID vs. DD/ID groups. **b** The results of neither k-means clustering nor t-SNE can distinguish the 3 patient groups from each other. ASD autism spectrum disorder, DD/ID developmental delay/intellectual disability.

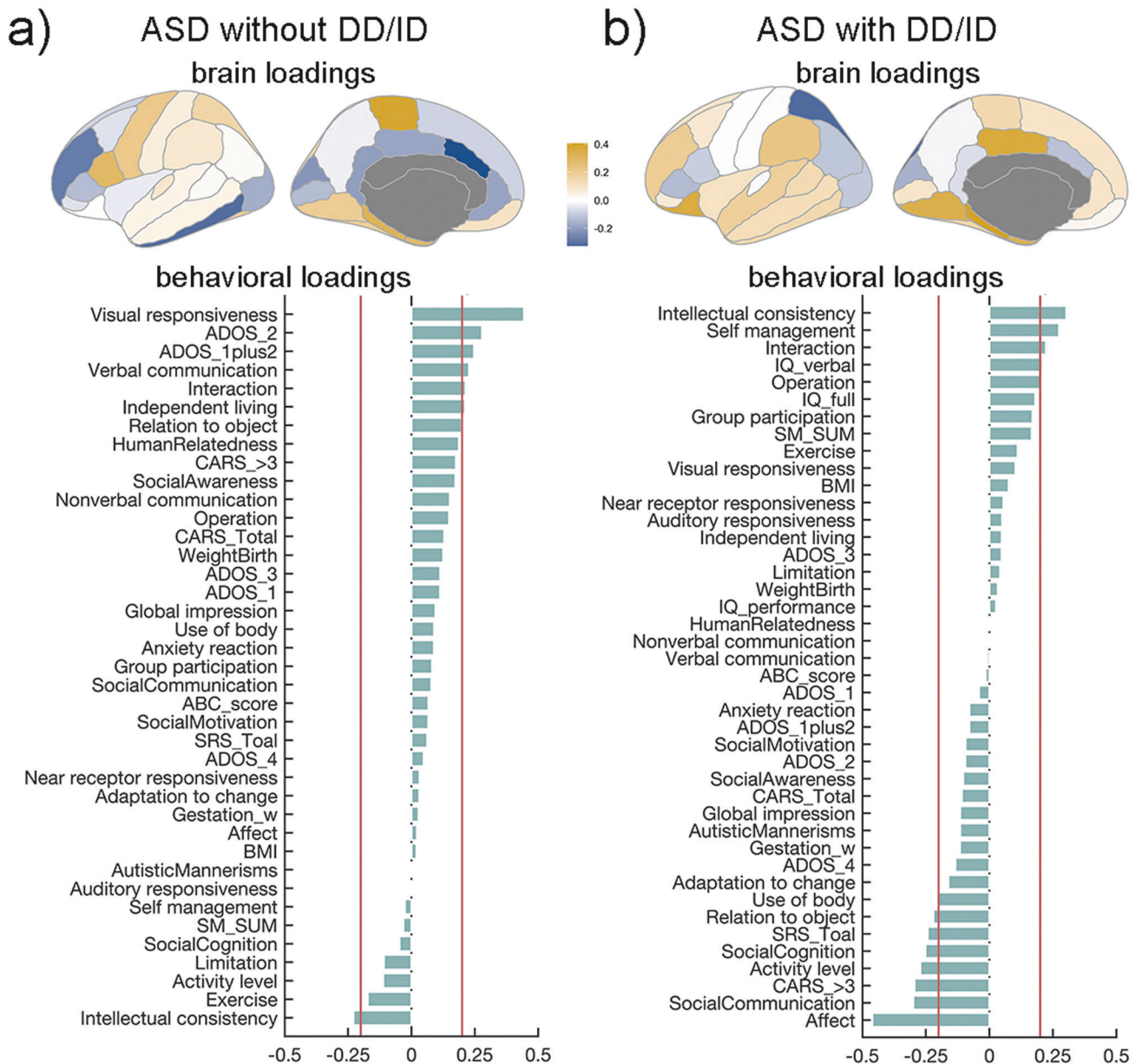


Fig. 4 The identified canonical modes linking GMV asymmetry deviations and behavioural performance in ASD children without DD/ID and ASD children with DD/ID. **a** The loadings of brain regions and ASD symptoms contributing to the canonical mode in ASD children without DD/ID. **b** The loadings of brain regions and ASD symptoms plus IQ contributing to the canonical mode in ASD children with DD/ID.

point was detected, indicating that the patient groups cannot be distinguished through the GMV asymmetry pattern (Fig. 3b). With the *t*-SNE method, we generated a spatial visualization of all individuals' asymmetry patterns through two-dimensional vectors, which confirmed that children of ASD with DD/ID, ASD without DD/ID and DD/ID cannot be differentiated from each other.

Associations between atypical asymmetry deviations and clinical symptoms

To understand the multiscale cascade in both the ASD and DD/ID populations, we conducted the canonical correlation analysis to explore the associations between brain structural asymmetry deviations and behavioural scores for ASD children without DD/ID, and ASD children with DD/ID respectively.

For ASD children without DD/ID, one significant multivariate association mode was detected between GMV asymmetry deviation maps with clinical scores ($r = 0.977$, $p_{\text{perm}} = 0.033$).

Setting the threshold of loading as ± 0.2 , we identified regions contributing to the canonical mode, including six regions with positive loadings (the paracentral gyrus, parahippocampal gyrus, inferior frontal gyrus pars opercularis, entorhinal, frontal pole and precentral gyrus) and four regions with negative loadings (the caudal anterior cingulate, inferior temporal gyrus, rostral middle frontal gyrus and cuneus). Contributed clinical measurements included the visual responsiveness, ADOS_2, the sum of ADOS_1 and ADOS_2, verbal communication, interaction, and independent living scores, which showed positive loadings, and intellectual consistency showed negative loads, as shown in Fig. 4. Here, positive canonical loading indicates the more leftward GMV asymmetry, the higher neuropsychological scores, and vice versa.

For ASD children with DD/ID, one significant canonical mode was identified linking the GMV asymmetry deviation maps with both clinical scores and IQ scores ($r = 0.988$, $p_{\text{perm}} = 0.003$). Eight brain regions positively contributed to the identified associations,

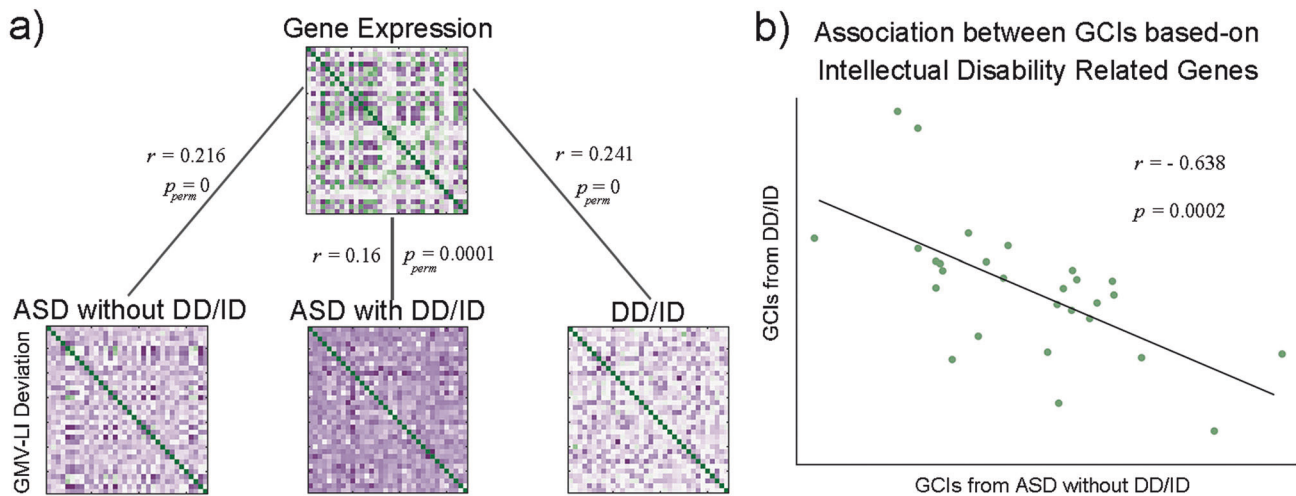


Fig. 5 Associations characterized by interregional similarities between gene expression profiles and GMV asymmetry deviations of patient groups. **a** Significant interregional similarities were found between transcriptional profiles and GMV asymmetry in each group. **b** The GCI values of intellectual disability-related genes were significantly negatively correlated between children with DD/ID only and ASD children without DD/ID. ASD autism spectrum disorder, DD/ID developmental delay/intellectual disability, GCI gene contribution index.

including the parahippocampal gyrus, posterior cingulate cortex, lateral orbitofrontal gyrus, lingual gyrus, entorhinal, temporal pole, supramarginal gyrus, and frontal pole. The superior parietal gyrus negatively contributed to the mode. For clinical and cognitive performances, intellectual consistency, self-management, interaction, verbal IQ and Operation showed positive contributions, while affect, social communication, CARS, activity level, social cognition, SRS, relation to object and the use of body showed negative contributions.

The canonical correlation analysis for the two ASD groups together did not yield any significant association modes.

Association between atypical asymmetry deviations and gene expression profiles

To quantify the multivariate association pattern between gene expression profiles and GMV asymmetry deviations for each group, we conducted the partial least squares regression. For the ASD with DD/ID group, three regression components significantly explained 20.6% ($r = 0.454$, $p = 0.007$), 14.7% ($r = 0.384$, $p = 0.025$) and 16% ($r = 0.4$, $p = 0.019$) of the response variables. For ASD without DD/ID group, only two regression components significantly explained the response variables: component two for 26.4% ($r = 0.39$, $p = 0.023$) and component three for 42.6% ($r = 0.402$, $p = 0.018$). However, none of these correlations survived after the spatial permutation tests ($N = 10000$, all $p_{perm} > 0.5$). Given that genes served as source factors, these results suggested that the associations between gene expression profiles and GMV asymmetry might be nonlinear.

Next, inter-regional similarity analysis was conducted to detect the significant associations between gene and brain profiles for each patient group. As shown in Fig. 5a, the associations in three groups were all significant (ASD children with DD/ID is: $r = 0.16$, $p_{perm} = 0.0001$; ASD children without DD/ID: $r = 0.216$, $p_{perm} = 0$; DD/ID children: $r = 0.241$, $p_{perm} = 0$). The gene contribution index (GCI) values of autism related genes and intellectual disability related genes were extracted according to the In Situ Hybridization gene lists. Correlations across groups were then calculated. We only found a significant negative correlation between the GCI values of intellectual disability related genes between the DD/ID and ASD without DD/ID groups ($r = -0.638$, $p < 0.001$, Fig. 5b).

The shared and specific genes and their terms of the three patient groups are shown with circle networks in Fig. 6a. Through multigene list meta-analysis, we identified the related functional terms or pathways to provide more information. Four Gene

Ontology (GO) terms were consistently enriched in the three patient groups for the expressions of genes associated with GMV asymmetry, including 'regulation of transmembrane transport', 'neuron projection development', 'axon', and 'supramolecular fiber organization' (FDR corrected $p < 0.05$, Fig. 6b). The GO term clusters identified in all ASD children were 'postsynapse' and 'brain development'. The GO terms 'cytoplasmic translation' and 'polymeric cytoskeletal fiber' were clustered together in both ASD with DD/ID and DD/ID groups. Furthermore, specific GO terms for ASD without DD/ID group included 'nuclear inner membrane', 'synapse organization', 'regulation of synapse pruning', 'response to salt', 'cytoplasmic side of membrane', 'kinase binding' and 'perinuclear region of cytoplasm'. Specific GO term for ASD with DD/ID children was 'regulation of neurotransmitter level'. Specific GO terms for DD/ID were 'cell adhesion molecule binding', 'cell projection assembly', and 'regionalization'. Figure 6c shows the proportion of each patient group relating to the enriched GO term clusters, and Fig. 6d shows the GO terms colored by cluster.

DISCUSSION

With normative models and GMV asymmetry measurement, this study explored the neuropathological mechanisms underlying the comorbidities and differentiations between young ASD and DD/ID children from a multiscale cascade perspective. We observed an ASD-common GMV rightward laterality pattern in the inferior parietal lobe and precentral gyrus, as well as abnormal heterogeneity in the temporal pole. Additionally, ASD children with DD/ID exhibited more regional abnormalities; ASD children without DD/ID showed higher within-group heterogeneity, while children with DD/ID showed no significant abnormality. The GMV laterality patterns of ASD children without DD/ID were associated with ASD symptoms only, whereas these of ASD children with DD/ID were associated with both ASD symptoms and verbal IQ. Lastly, the GMV asymmetry patterns of children with ASD without DD/ID, ASD with DD/ID, and DD/ID only were associated with both shared and unique gene expression profiles.

Employing normative models, we detected significant abnormality in the inferior parietal lobe and precentral gyrus with more rightward laterality, and in the temporal pole with increased individual variability of ASD children both with and without DD/ID. Previous studies revealed that the inferior parietal lobe involved in visuospatial processing [57, 58], the precentral gyrus supporting sensorimotor functions, and the temporal pole involved in

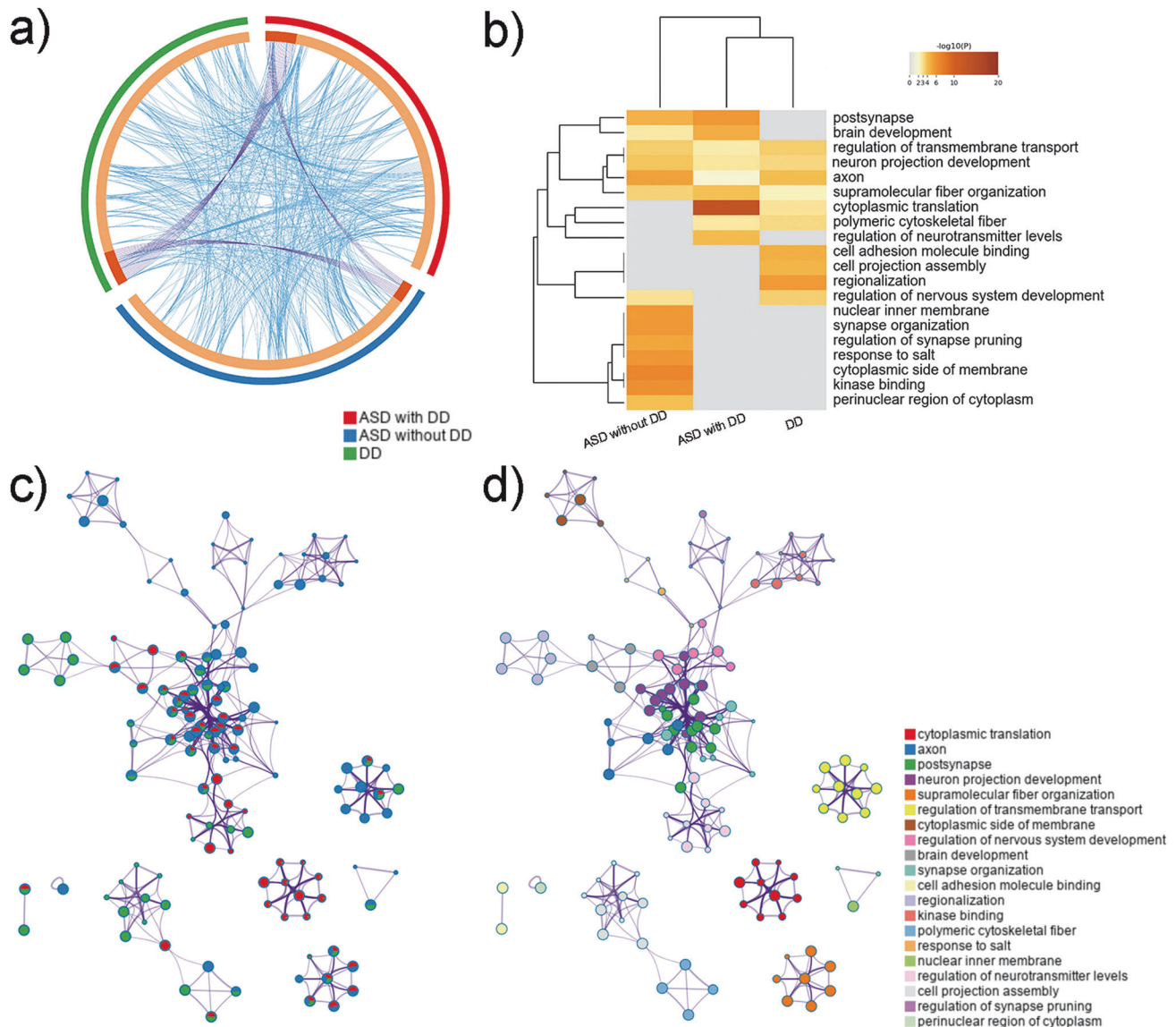


Fig. 6 Functional enrichment of GMV asymmetry-related multiple gene lists from ASD children with DD, ASD children without DD and children with DD only. **a** The shared and specific genes and their GO terms among patient groups. Orange represents genes in each patient group. Purple curves indicate identical genes between the two groups. Blue links show the same terms in which genes from the two groups were enriched. **b** The top 20 clusters for enriched GO terms from all patient groups, corrected by FDR $p < 0.05$. **c** The GO term network characterized by pie charts. One circle represents an enriched term. The proportional coloured pie shows the percentage of genes from one patient group in all groups; red indicates ASD children with DD/ID, blue represents ASD children without DD/ID and green indicates children with DD/ID only. **d** The GO term network characterized by clusters. The same as (c), but the colour of the circles indicates clusters. ASD autism spectrum disorder, DD/ID developmental delay/intellectual disability, GO Gene Ontology.

individual differences in sensory processing [59, 60], semantic representations [61], and social and emotional cognition [62]. The abnormality of those cognitive functions were core deficits in ASD populations, indicating that we successfully captured the specific alterations in brain structure laterality of young ASD children. Previous studies usually employed the group-level analysis and reported inconsistent or no significant regional GMV asymmetry in ASD population [39, 63, 64]. Here, we calculated the GMV asymmetry based on deviations from normative models, which have shown potentials in evaluating individual performance and disease heterogeneity [65–68]. Additionally, this work focused on young children with a relatively narrow age range, which minimized the effects of development and its complex interactions with environment on disease. Notably, no significant deviations of GMV asymmetry were found in children with DD/

ID, which might be because that DD/ID involves impairments in multiple cognitive processes, including both the left and right brain systems, resulting in very little overall asymmetry changes [68].

The GMV asymmetry deviation patterns of ASD children with DD/ID showed high similarities with both ASD without DD/ID and DD/ID children, whereas no significant correlation was found between the ASD without DD/ID and DD/ID children. These results indicated that the brain structural abnormalities induced from the ASD might be different from the DD/ID. Additionally, we also revealed the similarities in whole-brain structural asymmetry patterns across the three patient groups, which cannot be separated from each other by unsupervised clustering. Aglinskas et al. [69] found that instead of distinct subtypes, ASD-common neuroanatomy variations are organized along a continuous

dimension. Our study echoed with this statement and indicated that the brain GMV asymmetry patterns of ASD without DD/ID, ASD with DD/ID, and DD/ID groups might be gradually differentiated in a continuum, with ASD with DD/ID group located in the middle.

The canonical correlation analysis identified multivariate correlations between brain GMV asymmetry deviations and autistic symptoms in the ASD without DD/ID group, whereas deviations in the ASD with DD/ID group were associated with both ASD symptoms and verbal IQ. With abnormal asymmetry in the parahippocampal, entorhinal, and frontal pole, involved in memory, exploiting and exploration functions [62], both ASD children with and without DD/ID showed serious communication and social impairments. Congruent with this, similar abnormal GMV asymmetry of the above brain regions and their links to social communication problems have been reported in previous studies [70–73]. Of note, no significant association was detected between brain GMV asymmetry and clinical phenotype in all ASD children. This indicates a potential inter-group heterogeneity between ASD children with normal and low cognitive ability, yielding a complex relationship between the brain asymmetry changes and clinical symptoms which couldn't be identified with linear analysis. Future studies using nonlinear algorithms to establish the links between brain measurements and clinical phenotypes might reveal the characteristics of ASD accurately.

GMV asymmetry related genes were enriched in the GO terms 'postsynapse' and 'brain development' in ASD children with and without DD/ID, suggesting the genetic effects microscale brain characteristics in ASD with evidences from many studies [74, 75]. We also revealed that the GO terms 'cytoplasmic translation' and 'polymeric cytoskeletal fiber' were associated with ASD children with DD/ID and DD/ID children, indicating these cellular dysfunctions affect brain morphology and drive complex intellectual delay phenotypes.

Some limitations of this study should be stated. Firstly, it is worth noting that GMV in current study is obtained by automated morphology method called voxel-based morphometry (VBM). The performances of segmentation and registration in preprocessing are key factors on accuracy of VBM. To overcome the potential VBM methodology confounders involved by systematically developmental and/or clinical effects, registration algorithm in state of the art, strict 2nd around quality control for segmentation, and validation for preprocessing were conducted. Future studies are expected to provide more convergent neuroimaging evidences on the lateralization alterations, especially in VBM-sensitive brain regions, in very young ASD children. Secondly, the normative model extracting GMV asymmetry deviations only considered the effects of age and sex. Environmental factors, such as socio-economic status, may also affect the brain morphology development [76, 77], which should be included in future studies. Thirdly, limited by the availability of gene expression data, we linked GMV asymmetry deviations in 1- to 7-year-old children to transcriptional profiles from healthy adults and employed the multivariate instead of univariate association methods. With the gradual establishment and improvement of ASD datasets including SAED cohort, follow-up analysis is expected to investigate the brain morphology-transcriptome association within the same ASD participants. Fourthly, the sex ratio of this work is unbalanced, which limits the exploration about sex effects on developmental disorders. We calculated the regional developmental curves of asymmetry for healthy males and females separately. Similar patterns were detected (see Supplementary Fig. S4). Meanwhile, we also calculated the GMV asymmetry deviation maps of males and females separately for the three patient groups to explore the sex effects on abnormality, shown in Supplementary Fig. S5. The group mean GMV asymmetry deviation maps were more similar with the maps of males in all the three patient groups, while the maps of females showed specific patterns in regions including

insular, precentral gyrus, and temporal-parietal junction regions. Those results indicated that the sex effects might be different between healthy and developmental disordered population, which should be explored in further with samples with more balanced sex ratio. Additionally, during the data collection, professional pediatricians made clinical assessments for cooperation to determine whether sedation would be used. For children with high cooperation, their MRI data was collected during natural sleep or awake is of priority. 2 of 563 ASD with DD/ID children, 1 of 212 ASD without DD/ID children, 1 of 36 DD/ID children and 21 of 219 TD children were scanned during natural sleep or awake without sedation. Most of our subjects were scanned during sedation-induced sleep. The proportions of sedation in ASD and DD/ID children are higher than that in TD group. It indicates the low adaptability in diagnosed group might account for pathological changes, which need to be further explored. Finally, functional brain variants also play an important role in the multimodal cascade, which may mediate the relations between the structural brain and the behavioural phenotype. The hierarchical associations with multimodality data from gene expression to brain structure, brain function, and finally clinical phenotypes should be explored in the further to elucidate the pathological mechanism of ASD heterogeneity and DD/ID.

In conclusion, we identified rightward asymmetry in the inferior parietal lobe and precentral gyrus, and higher individual variability in temporal pole in ASD children. In addition, ASD with DD/ID children have more extensive abnormality in asymmetry deviation values (e.g., the precuneus, SMA, medial prefrontal gyrus); ASD without DD/ID children have more extensive abnormality in asymmetry individual variability (e.g., the parahippocampal gyrus, fusiform, and medial orbitofrontal gyrus); and children with DD/ID only showed no significant abnormality in asymmetry. The GMV laterality patterns of ASD without DD/ID children were associated with ASD symptoms, whereas those of ASD with DD/ID children were associated with both ASD symptoms and verbal IQ. Finally, the GMV laterality of all patient groups was significantly associated with shared and unique gene expression profiles. Our findings revealed the potency of brain asymmetry as a mediator variable for multiscale cascade analysis in developmental disorders and provides insights to the potential neural mechanisms.

DATA AVAILABILITY

Access to the identified participant research data must be approved by the research ethics board on a case-by-case basis, please contact the corresponding authors (feili@shsmu.edu.cn, mcao@fudan.edu.cn) for assistance in data access request.

CODE AVAILABILITY

The code for spatial autocorrelation-preserving permutation test is available at (https://github.com/frantisekvasa/rotate_parcellation) (version 3, June 2022). All home developed codes will be given on request.

REFERENCES

1. Edition F. Diagnostic and statistical manual of mental disorders. Am Psychiatr Assoc. 2013;21:591–643.
2. Lombardo MV, Lai M-C, Baron-Cohen S. Big data approaches to decomposing heterogeneity across the autism spectrum. *Mol Psychiatry*. 2019;24:1435–50.
3. Li H-H, Feng J-Y, Wang B, Zhang Y, Wang C-X, Jia F-Y. Comparison of the children neuropsychological and behavior scale and the Griffiths mental development scales when assessing the development of children with autism. *Psychol Res Behav Manag*. 2019;12:973–81.
4. McDonald NM, Senturk D, Scheffler A, Brian JA, Carver LJ, Charman T, et al. Developmental trajectories of infants with multiplex family risk for autism: a baby siblings research consortium study. *JAMA Neurol*. 2020;77:73–81.
5. Srouf M, Shevell M. Genetics and the investigation of developmental delay/intellectual disability. *Arch Dis Child*. 2014;99:386–9.
6. Shevell M, Ashwal S, Donley D, Flint J, Gingold M, Hirtz D, et al. Practice parameter: evaluation of the child with global developmental delay [RETIRED]: report

- of the quality standards subcommittee of the american academy of neurology and the practice committee of the child neurology society. *Neurology*. 2003;60:367–80.
7. Courchesne E, Pramparo T, Gazestani VH, Lombardo MV, Pierce K, Lewis NE. The ASD living Biology: from cell proliferation to clinical phenotype. *Mol Psychiatry*. 2019;24:88–107.
 8. Lombardo MV, Pramparo T, Gazestani V, Warrier V, Bethlehem RA, Carter Barnes C, et al. Large-scale associations between the leukocyte transcriptome and BOLD responses to speech differ in autism early language outcome subtypes. *Nat Neurosci*. 2018;21:1680–8.
 9. Courchesne E, Gazestani VH, Lewis NE. Prenatal origins of ASD: the when, what, and how of ASD development. *Trends Neurosci*. 2020;43:326–42.
 10. Gazestani VH, Chiang AW, Courchesne E, Lewis NE. Autism genetics perturb prenatal neurodevelopment through a hierarchy of broadly-expressed and brain-specific genes. *bioRxiv*. 2020:2020.05. 23.112623.
 11. Hyman SL, Levy SE, Myers SM, Kuo DZ, Apkon S, Davidson LF, et al. Identification, evaluation, and management of children with autism spectrum disorder. *Pediatrics*. 2020;145:e20193447.
 12. Gilmore JH, Knickmeyer RC, Gao W. Imaging structural and functional brain development in early childhood. *Nat Rev Neurosci*. 2018;19:123–37.
 13. Cao M, Huang H, He Y. Developmental connectomics from infancy through early childhood. *Trends Neurosci*. 2017;40:494–506.
 14. Brouwer RM, van Haren NE, Forti MD, van den Berg LH, Penninx BW, Falkai PG, et al. Dynamics of brain structure and its genetic architecture over the lifespan. *Strukturelle und funktionelle Organisation des Gehirns*; 2020.
 15. Gottesman II, Hanson DR. Human development: biological and genetic processes. *Annu Rev Psychol*. 2005;56:263–86.
 16. Parikshak NN, Gandal MJ, Geschwind DH. Systems biology and gene networks in neurodevelopmental and neurodegenerative disorders. *Nat Rev Genet*. 2015;16:441–58.
 17. Güntürkün O, Ströckens F, Ocklenburg S. Brain lateralization: a comparative perspective. *Physiol Rev*. 2020;100:1019–63.
 18. Wang J, Ma S, Yu P, He X. Evolution of human brain left–right asymmetry: old genes with new functions. *Mol Biol Evol*. 2023;40:msad181.
 19. Roe JM, Vidal-Pineiro D, Amlien IK, Pan M, Sneve MH, de Schotten MT, et al. Tracing the development and lifespan change of population-level structural asymmetry in the cerebral cortex. *Elife*. 2023;12:e84685.
 20. Carrion-Castillo A, Pepe A, Kong X-Z, Fisher SE, Mazoyer B, Tzourio-Mazoyer N, et al. Genetic effects on planum temporale asymmetry and their limited relevance to neurodevelopmental disorders, intelligence or educational attainment. *Cortex*. 2020;124:137–53.
 21. Kong X-Z, Postema M, Schijven D, Castillo AC, Pepe A, Crivello F, et al. Large-scale phenomic and genomic analysis of brain asymmetrical skew. *Cereb Cortex*. 2021;31:4151–68.
 22. Sha Z, Schijven D, Carrion-Castillo A, Joliot M, Mazoyer B, Fisher SE, et al. The genetic architecture of structural left–right asymmetry of the human brain. *Nat Hum Behav*. 2021;5:1226–39.
 23. Ratnarajah N, Rifkin-Graboi A, Fortier MV, Chong YS, Kwek K, Saw S-M, et al. Structural connectivity asymmetry in the neonatal brain. *Neuroimage*. 2013;75:187–94.
 24. Scheinost D, Lacadie C, Vohr BR, Schneider KC, Papademetris X, Constable RT, et al. Cerebral lateralization is protective in the very prematurely born. *Cereb Cortex*. 2015;25:1858–66.
 25. Habas PA, Scott JA, Roosta A, Rajagopalan V, Kim K, Rousseau F, et al. Early folding patterns and asymmetries of the normal human brain detected from in utero MRI. *Cereb Cortex*. 2012;22:13–25.
 26. Kaspran G, Langs G, Brugger PC, Bittner M, Weber M, Arantes M, et al. The prenatal origin of hemispheric asymmetry: an in utero neuroimaging study. *Cereb Cortex*. 2011;21:1076–83.
 27. Dubois J, Hertz-Pannier L, Cachia A, Mangin J-F, Le Bihan D, Dehaene-Lambertz G. Structural asymmetries in the infant language and sensori-motor networks. *Cereb Cortex*. 2009;19:414–23.
 28. Li G, Nie J, Wang L, Shi F, Lyall AE, Lin W, et al. Mapping longitudinal hemispheric structural asymmetries of the human cerebral cortex from birth to 2 years of age. *Cereb Cortex*. 2014;24:1289–1300.
 29. Koelkebeck K, Miyata J, Kubota M, Kohl W, Son S, Fukuyama H, et al. The contribution of cortical thickness and surface area to gray matter asymmetries in the healthy human brain. *Hum Brain Mapp*. 2014;35:6011–22.
 30. Gracia-Tabuenca Z, Moreno MB, Barrios FA, Alcauter S. Hemispheric asymmetry and homotopy of resting state functional connectivity correlate with visuospatial abilities in school-age children. *Neuroimage*. 2018;174:441–8.
 31. Song JW, Mitchell PD, Kolasinski J, Ellen Grant P, Galaburda AM, Takahashi E. Asymmetry of white matter pathways in developing human brains. *Cereb Cortex*. 2015;25:2883–93.
 32. Shu N, Liu Y, Duan Y, Li K. Hemispheric asymmetry of human brain anatomical network revealed by diffusion tensor tractography. *BioMed Res Int*. 2015;2015:908917.
 33. Zhong S, He Y, Shu H, Gong G. Developmental changes in topological asymmetry between hemispheric brain white matter networks from adolescence to young adulthood. *Cereb Cortex*. 2017;27:2560–70.
 34. Karolis VR, Corbetta M, Thiebaut de Schotten M. The architecture of functional lateralisation and its relationship to callosal connectivity in the human brain. *Nat Commun*. 2019;10:1–9.
 35. Kleinhans NM, Müller R-A, Cohen DN, Courchesne E. Atypical functional lateralization of language in autism spectrum disorders. *Brain Res*. 2008;1221:115–25.
 36. Joseph RM, Fricker Z, Fenoglio A, Lindgren KA, Knaus TA, Tager-Flusberg H. Structural asymmetries of language-related gray and white matter and their relationship to language function in young children with ASD. *Brain Imaging Behav*. 2014;8:60–72.
 37. Floris DL, Lai MC, Auer T, Lombardo MV, Ecker C, Chakrabarti B, et al. Atypically rightward cerebral asymmetry in male adults with autism stratifies individuals with and without language delay. *Hum Brain Mapp*. 2016;37:230–53.
 38. Lindell AK, Hudry K. Atypicalities in cortical structure, handedness, and functional lateralization for language in autism spectrum disorders. *Neuropsychol Rev*. 2013;23:257–70.
 39. Postema MC, Van Rooij D, Anagnostou E, Arango C, Auzias G, Behrmann M, et al. Altered structural brain asymmetry in autism spectrum disorder in a study of 54 datasets. *Nat Commun*. 2019;10:1–12.
 40. Dai Y, Liu Y, Zhang L, Ren T, Wang H, Yu J, et al. Shanghai autism early development: an integrative Chinese ASD cohort. *Neurosci Bull*. 2022;38:1603–7.
 41. Zhao T, Liao X, Fonov VS, Wang Q, Men W, Wang Y, et al. Unbiased age-specific structural brain atlases for Chinese pediatric population. *Neuroimage*. 2019;189:55–70.
 42. Desikan RS, Ségonne F, Fischl B, Quinn BT, Dickerson BC, Blacker D, et al. An automated labeling system for subdividing the human cerebral cortex on MRI scans into gyral based regions of interest. *Neuroimage*. 2006;31:968–80.
 43. Fortin J-P, Parker D, Tunç B, Watanabe T, Elliott MA, Ruparel K, et al. Harmonization of multi-site diffusion tensor imaging data. *Neuroimage*. 2017;161:149–70.
 44. Fortin J-P, Cullen N, Sheline YI, Taylor WD, Aselcioglu I, Cook PA, et al. Harmonization of cortical thickness measurements across scanners and sites. *Neuroimage*. 2018;167:104–20.
 45. Johnson WE, Li C, Rabinovic A. Adjusting batch effects in microarray expression data using empirical Bayes methods. *Biostatistics*. 2007;8:118–27.
 46. Rutherford S, Kia SM, Wolfers T, Frazz C, Zabih M, Dinga R, et al. The normative modeling framework for computational psychiatry. *Nature protocols*. 2022;17:1711–34.
 47. Burt JB, Helmer M, Shinn M, Anticevic A, Murray JD. Generative modeling of brain maps with spatial autocorrelation. *Neuroimage*. 2020;220:117038.
 48. Váša F, Seidlitz J, Romero-García R, Whitaker KJ, Rosenthal G, Vértes PE, et al. Adolescent tuning of association cortex in human structural brain networks. *Cereb Cortex*. 2018;28:281–94.
 49. Hawrylycz MJ, Lein ES, Guillozet-Bongaarts AL, Shen EH, Ng L, Miller JA, et al. An anatomically comprehensive atlas of the adult human brain transcriptome. *Nature*. 2012;489:391–9.
 50. Arnatkevičiūtė A, Fulcher BD, Fornito A. A practical guide to linking brain-wide gene expression and neuroimaging data. *Neuroimage*. 2019;189:353–67.
 51. Abdi H. Partial least squares regression and projection on latent structure regression (PLS Regression). *Wiley Interdiscip Rev Comput Stat*. 2010;2:97–106.
 52. Romero-García R, Seidlitz J, Whitaker KJ, Morgan SE, Fonagy P, Dolan RJ, et al. Schizotypy-related magnetization of cortex in healthy adolescence is colocalized with expression of schizophrenia-related genes. *Biol Psychiatry*. 2020;88:248–59.
 53. Xie Y, Xu Z, Xia M, Liu J, Shou X, Cui Z, et al. Alterations in connectome dynamics in autism spectrum disorder: a harmonized mega-and meta-analysis study using the autism brain imaging data exchange dataset. *Biol Psychiatry*. 2022;91:945–55.
 54. Morgan SE, Seidlitz J, Whitaker KJ, Romero-García R, Clifton NE, Scarpazza C, et al. Cortical patterning of abnormal morphometric similarity in psychosis is associated with brain expression of schizophrenia-related genes. *Proc Natl Acad Sci USA*. 2019;116:9604–9.
 55. Li J, Seidlitz J, Suckling J, Fan F, Ji G-J, Meng Y, et al. Cortical structural differences in major depressive disorder correlate with cell type-specific transcriptional signatures. *Nat Commun*. 2021;12:1–14.
 56. Yeo BT, Krienen FM, Chee MW, Buckner RL. Estimates of segregation and overlap of functional connectivity networks in the human cerebral cortex. *Neuroimage*. 2014;88:212–27.
 57. Silk TJ, Rinehart N, Bradshaw JL, Tonge B, Egan G, O’Boyle MW, et al. Visuospatial processing and the function of prefrontal-parietal networks in autism spectrum disorders: a functional MRI study. *Am J Psychiatry*. 2006;163:1440–3.

58. Rolls ET, Deco G, Huang C-C, Feng J. The human posterior parietal cortex: effective connectome, and its relation to function. *Cereb Cortex*. 2023;33:3142–70.
59. Yoshimura S, Sato W, Kochiyama T, Uono S, Sawada R, Kubota Y, et al. Gray matter volumes of early sensory regions are associated with individual differences in sensory processing. *Hum Brain Mapp*. 2017;38:6206–17.
60. Rolls ET, Deco G, Huang C-C, Feng J. Multiple cortical visual streams in humans. *Cereb Cortex*. 2023;33:3319–49.
61. Rolls ET, Deco G, Huang C-C, Feng J. The human language effective connectome. *NeuroImage*. 2022;258:119352.
62. Rolls ET. *Brain computations and connectivity*. Oxford University Press; 2023.
63. Fu L, Wang Y, Fang H, Xiao X, Xiao T, Li Y, et al. Longitudinal study of brain asymmetries in autism and developmental delays aged 2–5 years. *Neuroscience*. 2020;432:137–49.
64. Sha Z, Van Rooij D, Anagnostou E, Arango C, Auzias G, Behrmann M, et al. Subtly altered topological asymmetry of brain structural covariance networks in autism spectrum disorder across 43 datasets from the ENIGMA consortium. *Mol Psychiatry*. 2022;27:2114–25.
65. Marquand AF, Rezek I, Buitelaar J, Beckmann CF. Understanding heterogeneity in clinical cohorts using normative models: beyond case-control studies. *Biol Psychiatry*. 2016;80:552–61.
66. Wolfers T, Beckmann CF, Hoogman M, Buitelaar JK, Franke B, Marquand AF. Individual differences v. the average patient: mapping the heterogeneity in ADHD using normative models. *Psychol Med*. 2020;50:314–23.
67. Chien Y-L, Lin H-Y, Tung Y-H, Hwang T-J, Chen C-L, Wu C-S, et al. Neurodevelopmental model of schizophrenia revisited: similarity in individual deviation and idiosyncrasy from the normative model of whole-brain white matter tracts and shared brain-cognition covariation with ADHD and ASD. *Mol Psychiatry*. 2022;27:3262–71.
68. Pigdon L, Willmott C, Reilly S, Conti-Ramsden G, Gaser C, Connelly A, et al. Gray matter volume in developmental speech and language disorder. *Brain Structure Funct*. 2019;224:3387–98.
69. Aglinskas A, Hartshorne JK, Anzellotti S. Contrastive machine learning reveals the structure of neuroanatomical variation within autism. *Science*. 2022;376:1070–4.
70. Yamasaki S, Yamasue H, Abe O, Suga M, Yamada H, Inoue H, et al. Reduced gray matter volume of pars opercularis is associated with impaired social communication in high-functioning autism spectrum disorders. *Biol Psychiatry*. 2010;68:1141–7.
71. Li C, Ning M, Fang P, Xu H. Sex differences in structural brain asymmetry of children with autism spectrum disorders. *J Integr Neurosci*. 2021;20:331–40.
72. Eisenberg IW, Wallace GL, Kenworthy L, Gotts SJ, Martin A. Insistence on sameness relates to increased covariance of gray matter structure in autism spectrum disorder. *Mol Autism*. 2015;6:1–12.
73. Rolls ET, Deco G, Huang C-C, Feng J. The connectivity of the human frontal pole cortex, and a theory of its involvement in exploit versus explore. *Cereb Cortex*. 2023;34:bhad416.
74. Indika N-LR, Deutz NE, Engelen MP, Peiris H, Wijetunge S, Perera R. Sulfur amino acid metabolism and related metabolites of autism spectrum disorder: a review of biochemical evidence for a hypothesis. *Biochimie*. 2021;184:143–57.
75. van Sadelhoff JH, Perez Pardo P, Wu J, Garssen J, Van Bergenhenegouwen J, Hogenkamp A, et al. The gut-immune-brain axis in autism spectrum disorders; a focus on amino acids. *Front Endocrinol*. 2019;10:247.
76. Brito NH, Noble KG. Socioeconomic status and structural brain development. *Front Neurosci*. 2014;8:276.
77. Rakesh D, Whittle S. Socioeconomic status and the developing brain—a systematic review of neuroimaging findings in youth. *Neurosci Biobehav Rev*. 2021;130:379–407.

ACKNOWLEDGEMENTS

This study was supported by grants from the National Natural Science Foundation of China (81901826, 61932008, 62076068, 82271627, 82125032, 81930095, 81761128035, 82202243, and 82204048), the Science and Technology Commission of Shanghai Municipality (23Y21900500, 19410713500 and 2018SHZDX01), the Shanghai Municipal Commission of Health and Family Planning (GWVI-11.1-34.GWV-10.1-XK07, 2020CXJQ01, 2018YJRC03), the Shanghai Clinical Key Subject Construction Project (shslczdzk02902), the Shanghai Municipal Science and Technology Major Project [2021ZD0200800, No.2018SHZDX01], Innovative research team of high-level local universities in Shanghai (SHSMU-ZDCX20211100), the Guangdong Key Project (2018B030335001), the Shanghai Municipal Commission of Health and Family Planning (20214Y0125), the National Key R&D Program of China (grant numbers 2018YFC1312900 and 2019YFA0709502), and the ZJ Lab, Shanghai Center for Brain Science and Brain-Inspired Technology and the 111 Project (grant number B18015).

AUTHOR CONTRIBUTIONS

MC, FL and SG designed the study. YD, YL, YZ, LD, ZC contributed to the acquisition of research data. SG and MC conducted the data analysis. FL, MC, and SG provided the interpretation of results. MC and SG wrote the first draft of the manuscript. ETR and JF revised the manuscript.

COMPETING INTERESTS

The authors declare no competing interests.

ETHICS APPROVAL AND CONSENT TO PARTICIPATE

The study was conducted in compliance with the declaration of Helsinki, approved by the Ethics Committee of Xinhua Hospital affiliated with the Shanghai Jiao Tong University School of Medicine (XHEC-C-2019-076) and registered with ClinicalTrials.gov (NCT04358744). The legal guardian of all participants signed the written informed consent after detailed information notification.

ADDITIONAL INFORMATION

Supplementary information The online version contains supplementary material available at <https://doi.org/10.1038/s41380-025-02890-9>.

Correspondence and requests for materials should be addressed to Fei Li or Miao Cao.

Reprints and permission information is available at <http://www.nature.com/reprints>

Publisher's note Springer Nature remains neutral with regard to jurisdictional claims in published maps and institutional affiliations.

Springer Nature or its licensor (e.g. a society or other partner) holds exclusive rights to this article under a publishing agreement with the author(s) or other rightsholder(s); author self-archiving of the accepted manuscript version of this article is solely governed by the terms of such publishing agreement and applicable law.